THE JOURNAL OF PHYSICAL CHEMISTRY B LETTERS

2005, *109,* 10538−10541
Published on Web 05/10/2005

Synthesis of Thermally Stable Highly Ordered Nanoporous Tin Oxide Thin Films with a 3D Face-Centered Orthorhombic Nanostructure

Vikrant N. Urade and Hugh W. Hillhouse*

School of Chemical Engineering, Purdue University, West Lafayette, Indiana 47907

Received: March 10, 2005; In Final Form: April 26, 2005

Thin films of nanoporous tin oxide with a 3D face-centered orthorhombic nanostructure have been synthesized by self-assembly that is controlled by post-coating thermal treatment under controlled humidity. In contrast to the conventional evaporation-induced self-assembly (EISA), the films here have no ordered nanostructure after dip-coating. However, the initial coatings are formed under conditions that inhibit significant hydrolysis and condensation for extended periods. This allows the use of postsynthesis thermal vapor treatments to completely control the formation of the nanostructure. With $EO_{106}-PO_{70}-EO_{106}$ (Pluronic F127) triblock copolymer as the template, highly ordered nanostructures were generated by exposing the disordered films to a stream of water vapor at elevated temperature, which rehydrates the films and allows the formation of the thermodynamically favored phase. Further exposure to water vapor drives the condensation reaction through the elimination of HCl. The X-ray diffraction pattern from the nanostructure was indexed in the space group *Fmmm* as determined by analysis of 2D small-angle X-ray scattering patterns at various angles of incidence. The nanostructure is then stabilized and made nanoporous by extended controlled thermal treatments. After self-assembly and template removal, the films are thermally stable up to 600 °C and retain an ordered, face-centered orthorhombic nanostructure.

Surfactant templated mesoporous materials[1] have attracted a great deal of attention in the chemical and materials science communities because of their promising potential applications in catalysis, separations, adsorption, and electronic (low-*k* dielectric, thermoelectric, photovoltaic, and optical) devices. The range of framework compositions has been extended from silica-based frameworks to non-silica transition metal oxides,[2−6] metals,[7] carbons,[8] and chalcogenides.[9] In particular, non-silica metal oxides with semiconducting properties such as titania, tin oxide and zinc oxide have promising applications in photovoltaic devices and sensors and as photocatalysts. The synthesis of such materials in highly ordered, mesoporous thin-film form is expected to open up interesting opportunities to enhance their efficiency and effectiveness for device applications.

Surfactant templated mesoporous titania thin films have been extensively investigated,[6,10] and it is now possible to reproducibly synthesize well-ordered thermally stable mesoporous titania thin films with crystalline walls.[11] However, there are relatively few reports of the synthesis of thermally stable ordered tin oxide materials, and most of these report either 2D hexagonal (plane group *p*6 or *p*6*mm*) or disordered structures. Pinnavaia et al. synthesized disordered wormhole-like tin oxide powders with nanocrystalline walls using neutral amine surfactants and tin(IV) isopropoxide as a precursor.[12] While these wormhole materials, prepared in powder form, have good access to the porosity, they do not have a well-defined mesostructure. Stucky and co-workers reported synthesis of 2D hexagonal tin oxide in powder form that was stable to calcination at 400 °C using poly(ethylene oxide)−poly(propylene oxide)−poly(ethylene oxide) (PEO−PPO−PEO) block copolymers as structure directing agents.[4] Later, Egashira and co-workers reported synthesis and gas-sensing properties of 2D hexagonal tin oxide powders using sodium stannate ($Na_2SnO_3 \cdot 3H_2O$) as the tin precursor and cationic cetylpyridinium chloride surfactants as the structure directing agent.[13] The resultant materials showed only a broad, low-intensity XRD peak after calcination at 600 °C. There are even fewer reports of thermally stable ordered tin oxide thin films. Zhou et al. reported synthesis and gas-sensing properties of mesostructured tin oxide thin films using PEO−PPO−PEO triblock copolymer templates.[14] The mesostructured tin oxide materials were reported to be sensitive to NO_2 gas levels as low as 1 ppm. However, the thermal stability of the materials was low, and after calcination at 300 °C, only a very broad peak was observed, indicating poor mesostructural order.

A new approach to synthesize mesostructured thin films of tin oxide with better mesoscale order was introduced by Miyata and co-workers.[15] The authors used a postsynthesis water vapor treatment at low temperature (40 °C) to synthesize highly ordered nanostructured tin oxide thin films. As-synthesized films (after dip-coating) were reported to be opaque with poor mesoscale ordering. However, after subjecting the films to water vapor, a disorder-to-order phase transition took place, resulting in the formation of a highly ordered 2D hexagonal nanostructure templated by either Brij58 or Brij76 surfactants. However, the authors did not demonstrate the removal of surfactant and the ability to yield a thermally stable mesoporous thin film. For many of the potential device applications such as sensors and solar cells, it will be necessary to remove the surfactant template

* Corresponding author. E-mail: hugh@purdue.edu. Telephone: 765-496-6056. Fax: 765-494-0805.

10.1021/jp051229+ CCC: $30.25

and enhance electronic transport properties of the framework. In particular, mesoporous phases of these materials having a 3D mesoporous network (as opposed to 2D) are of interest in order to fabricate ordered interpenetrated nanocomposite materials.

Here, we report the synthesis of thin films of mesoporous tin oxide having a 3D face-centered orthorhombic nanostructure using a postsynthesis water vapor treatment at elevated temperatures. In a typical synthesis, anhydrous tin(IV) chloride and deionized water are added to a solution of Pluronic F127 triblock copolymer ($HO(CH_2CH_2O)_n-(CH_2CH(CH_3)O)_m-(CH_2CH_2O)_nH$; $n = 106$, $m = 70$) in ethyl alcohol with an overall molar ratio of 1 $SnCl_4$:(5.0−10) × 10^{-3} F127:35−50 EtOH:10−20 H_2O to form the coating solution. Upon mixing, a highly exothermic reaction occurs, and the solution becomes warm. The coating solution is stirred at room temperature for 30 min, upon which it is stable for at least 4 months at room temperature, indicating that condensation is inhibited under these conditions. Thin films are then prepared by dip-coating on glass, quartz, silicon wafers, or conducting glass substrates (indium−tin oxide or F-doped tin oxide) at a withdrawal speed of 1 mm/s. Depending on the relative humidity during dip-coating and the subsequent drying period, the films were either opaque (relative humidity about 30% or higher) or transparent (relative humidity less than 30%). Regardless of opacity, the as-prepared films did not show any peak in the small-angle X-ray diffraction (XRD) pattern, indicating the lack of any long-range order. The films were dried at room temperature for 12−24 h, after which they were subjected to a water vapor atmosphere (relative humidity about 80% or more) at temperatures ranging from 30 to 70 °C for a period ranging from 30 min to 48 h. This humidity treatment, hereinafter referred to as the delayed humidity treatment (DHT), results in a disorder-to-order transition, leading to the formation of a highly ordered nanostructure. After the DHT, films are stable to changes in temperature and humidity. However, films calcined immediately after the DHT show complete collapse of the mesostructure even at temperatures as low as 250 °C, indicating that the inorganic framework is not fully condensed after the DHT. Films synthesized according to Miyata[15] also collapse upon a standard calcination ramp (1 °C/min) up to 400 °C. To drive the condensation and consolidate the inorganic walls, a thermal treatment at progressively higher temperatures with a very gradual increase in temperature was employed. A typical thermal treatment consists of heating at temperatures ranging from 50 to 250 °C with a 30 °C step and a residence of 10−12 h at each temperature. After the thermal treatment, the films were calcined in air at temperatures up to 600 °C for 4−6 h with a ramp of 3 °C/minute.

The symmetry and long-range order of the nanostructure of the films after DHT was determined using SAXS at a number of different angles of incidence, from 90° to grazing angles; see Figure 1. When the incident X-ray beam is perpendicular to the substrate (angle of incidence of 90°), a diffuse isotropic ring is observed. However, for SAXS at lower angles of incidence, spot patterns are observed. This indicated a highly ordered nanostructure that has a unit cell with domains that are highly oriented in one plane (the plane of the substrate) but sample many rotational orientations within that plane. The spot patterns at various angles of incidence were simulated using NANOCELL,[16] a Mathematica-based program for predicting SAXS and grazing incidence SAXS (GISAXS) patterns from nanostructured materials with specific models of disorder. From these simulations, the highest-symmetry space group commensurate with the SAXS patterns is face-centered orthorhombic

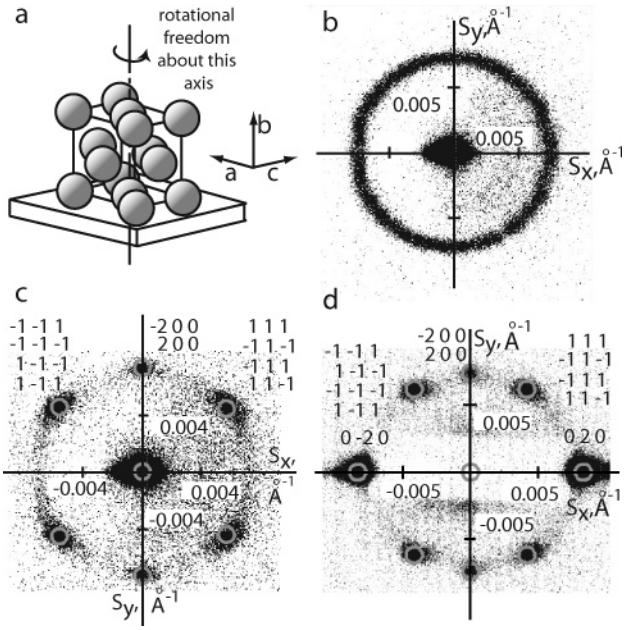

Figure 1. Unit cell of orthorhombic *Fmmm* mesostructure used for simulations in NANOCELL (a). The orientation of the mesostructure relative to the substrate is shown. (b) Small-angle X-ray scattering (SAXS) pattern of mesostructured thin films after the DHT with incidence normal to the substrate. The occurrence of a ring indicates that lattice vectors *a* and *c* have no preferred orientation in the plane parallel to the substrate. (c, d) SAXS patterns of mesostructured films after the DHT with the incident X-rays at 45° (c) and 2.5° (d) to the substrate. The overlaying circles are the locations of Bragg reflections as predicted using NANOCELL. Very good agreement is obtained between actual and predicted patterns using $a = 287$ Å, $b = 241$ Å, and $c = 217$ Å.

Fmmm (SG#69). The space group was determined by first noting that the structure directing agent used in the synthesis, Pluronic F127, has a very broad region in its binary temperature-concentration phase diagram over which a body-centered cubic phase is obtained.[17] Further, BCC cubic *Im*-3*m* mesostructures have been reported using this same template.[18] Upon compression during drying, it is expected that cubic symmetry will be broken and that the film will be described by a space group that has a subset of the symmetry elements in *Im*-3*m*. Therefore, we focused on subgroups of *Im*-3*m*. Similar reductions of symmetry upon compression normal to the substrate have been reported in the literature for 2D hexagonal *p*6*m* mesostructures, giving rise to a centered rectangular *c*2*m* structure,[5] and other (111) oriented cubic structures, giving rise to a (111) oriented rhombohedral *R*-3*m* structure.[19] While the SAXS patterns could not be described by *I*4/*mmm*, *Fmmm* is the highest-symmetry space group that fits the observed SAXS patterns. It should be noted that the non-isomorphic subgroups of *Fmmm*, such as *Fmm*2 or *F*222 or *C*2/*m*, can also be made to fit the observed data, but *Fmmm* is chosen because of its higher symmetry. As a result, *Fmmm* should be considered as an upper limit for the symmetry of the nanostructure after the compression that occurs upon drying. Very good fit was obtained with the observed patterns using lattice constants of $a = 287$ Å, $b = 241$ Å, and $c = 215$ Å of a [010] oriented *Fmmm* nanostructure with no preferred orientation of the *a* and *c* lattice vectors in the plane of the substrate (Figure 1a). SAXS patterns for incidence angles of 45° and 2.5° are shown in Figure 1c and d, respectively, with patterns simulated using NANOCELL overlaid. Mesoporous silica thin films with a similar face-centered orthorhombic symmetry prepared using the same structure directing agent (Pluronic F127) have also been reported in the literature.[20]

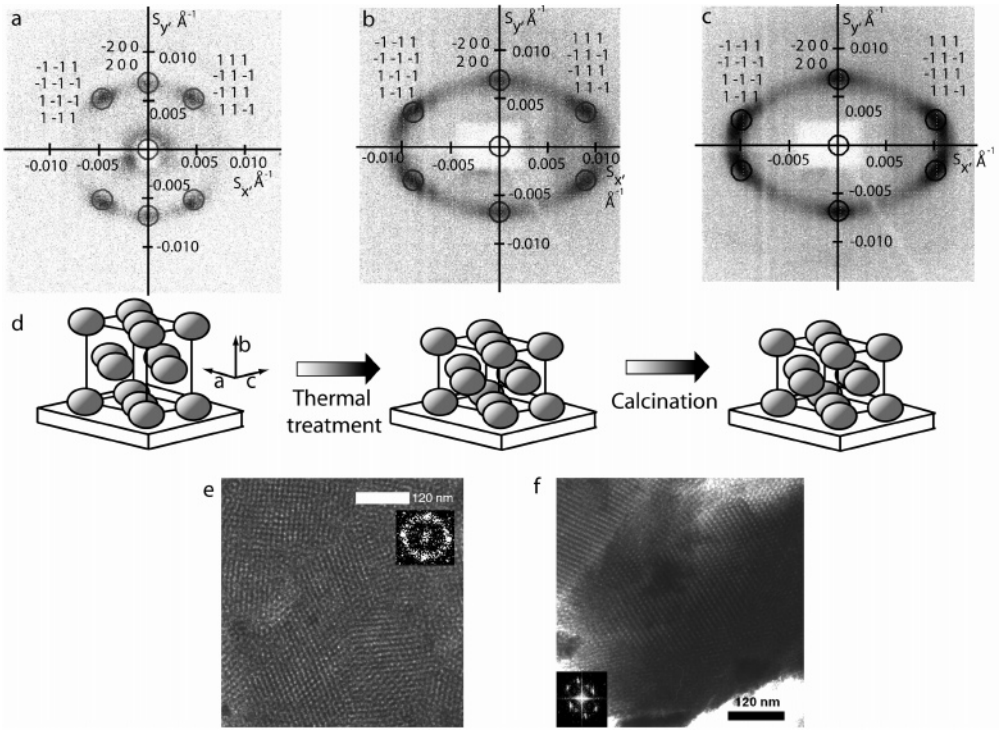

Figure 2. SAXS patterns of mesostructured tin oxide films after the DHT at 70 °C (a), an extended thermal treatment at temperatures up to 250 °C (b), and after calcination at 600 °C (c) with the incident X-rays at 30° with the plane of the substrate. The appearance of well-defined Bragg spots indicates that the mesostructure is preserved even after calcination at 600 °C. The changes seen in the SAXS pattern after the thermal treatment and calcination can be completely described by a reduction in the length of the *b* vector (d). Overlaid circles in (a), (b), and (c) are locations of Bragg reflections predicted using NANOCELL. Excellent agreement between predicted and actual patterns is seen with $b = 241$ Å after the DHT, 127 Å after thermal treatment, and 112 Å after calcination and $a = 287$ Å and $c = 217$ Å for all three cases. (e, f) TEM micrographs of calcined films. The presence of ordered domains in TEM images confirms the preservation of mesostructure.

The ordered structure of the films is retained through the progressive thermal treatments. These thermal treatments at temperatures less than 250 °C enhance the rate of condensation of the inorganic framework without removing the template, thus preserving the mesostructure. However, to ensure complete condensation, a residence time of 5−6 days at elevated temperatures was found to be necessary. Once the inorganic framework is completely condensed, the surfactant can be removed by calcination at temperatures up to 600 °C. The changes seen in the SAXS patterns after the thermal treatment and after calcination can be completely described by a reduction in the value of lattice constant *b*, with no change in lattice constants *a* or *c*, indicating that condensation is accompanied by unidirectional contraction of the mesostructure perpendicular to the substrate (Figure 2). The value of the lattice constant *b* decreases from 241 Å after the DHT to 127 Å after an extended thermal treatment at temperatures up to 250 °C. After surfactant removal by calcination at 600 °C, there is very small additional contraction of the mesostructure, and the lattice constant *b* decreases to 112 Å. Thus, about 89% of the total contraction of the mesostructure takes place during the extended thermal treatment, while calcination accounts for the remaining 11%. This indicates that condensation is practically complete during the extended thermal treatment, and calcination amounts to simply removal of the organics with little additional contraction. SAXS patterns after the DHT, thermal treatment at temperatures up to 250 °C, and calcination at 600 °C at a 30° angle of incidence are shown in Figure 2a−d, along with a schematic illustrating the changes in mesostructure that accompany these processing steps. The overlaying circles are the positions of Bragg reflections calculated using NANOCELL. Figure 2e,f shows representative transmission electron micrographs after the removal of surfactant.

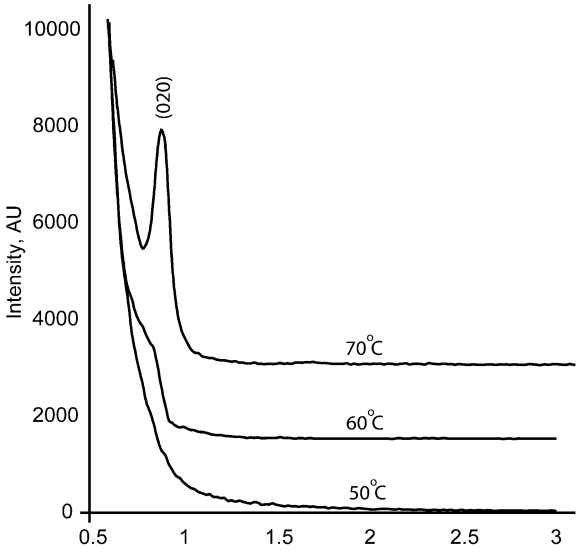

Figure 3. Effect of the temperature of the humidity treatment on mesostructure. 1D-SAXS patterns taken after a $3^1/_2$ h long DHT at 50, 60, and 70 °C. Temperature has a significant impact on the mesostructure obtained after the DHT, with higher temperatures favoring more ordered structures.

In this report, it is demonstrated that temperature has a dramatic effect on the disorder-to-order transition taking place during the DHT. Figure 3 shows the 1D XRD patterns for films on glass substrates treated at different DHT temperatures for a Pluronic F127:$SnCl_4$ molar ratio of 0.011. While no peak is seen for films treated at 50 °C, only an unresolved plateau is seen for films treated at 60 °C. At 70 °C, a high-intensity narrow

peak is seen (fwhm = 0.07°), indicating the formation of a highly ordered nanostructure.

In principle, this dramatic dependence of mesostructure order on the temperature of the DHT may involve several factors, including (1) kinetics of reorganization and assembly, (2) kinetics of hydrolysis and condensation, and (3) thermodynamic effects due to changes in the polarity of the PEO groups with temperature. However, it is clear that the self-assembly process reported here is not EISA.[21] In EISA, the self-assembly takes place right after dip-coating as the solvent evaporates, whereas in the present synthesis, solvent (water) is added into the films during the high-temperature, high-humidity DHT and self-assembly is induced by changing the polarity of the surfactant relative to that of the solvent. The mesostructure is formed while the films are still in the high-humidity environment, in the presence of excess water incorporated during the DHT. In situ GISAXS studies during DHT are currently underway to investigate further the key features of the mechanism of mesostructure assembly for these technologically important nanoporous films.

In summary, highly ordered films of 3D mesoporous tin oxide with an *Fmmm* structure have been synthesized using a postsynthesis water vapor treatment at elevated temperatures followed by careful thermal treatments to stabilize the structure. The resulting films are stable to surfactant removal by calcination at temperatures up to 600 °C.

Acknowledgment. The authors wish to acknowledge financial support from the National Science Foundation under the CAREER Award (0134255-CTS) and the Purdue Research Foundation (PRF-6904009). In addition, small-angle X-ray scattering data were collected utilizing the center for In-Situ X-ray Scattering from Nanomaterials and Catalysts at Purdue University supported by the National Science Foundation MRI program under the award 0321118-CTS. The authors also wish to acknowledge Debra Sherman and the Life Sciences Microscopy Facility at the Purdue University for assistance with TEM imaging.

References and Notes

(1) Beck, J. S.; Vartuli, J. C.; Roth, W. J.; Leonowicz, M. E.; Kresge, C. T.; Schmitt, K. D.; Chu, C. T. W.; Olson, D. H.; Sheppard, E. W.; McCullen, S. B.; Higgins, J. B.; Schlenker, J. L. *J. Am. Chem. Soc.* **1992**, *114*, 10834.

(2) Ciesla, U.; Demuth, D.; Leon, R.; Petroff, P.; Stucky, G.; Unger, K.; Schuth, F. *J. Chem. Soc., Chem. Commun.* **1994**, 1387.

(3) Huo, Q. S.; Margolese, D. I.; Ciesla, U.; Feng, P. Y.; Gier, T. E.; Sieger, P.; Leon, R.; Petroff, P. M.; Schuth, F.; Stucky, G. D. *Nature (London)* **1994**, *368*, 317.

(4) Yang, P. D.; Zhao, D. Y.; Margolese, D. I.; Chmelka, B. F.; Stucky, G. D. *Chem. Mater.* **1999**, *11*, 2813.

(5) Crepaldi, E. L.; Soler-Illia, G.; Grosso, D.; Albouy, P. A.; Amenitsch, H.; Sanchez, C. Design of transition metal oxide mesoporous thin films. In *Nanoporous Materials III*; Sayari, A.; Jaroniec, M., Eds.; Elsevier Science B.V.: Amsterdam, The Netherlands, 2002; Vol. 141, p 235.

(6) Crepaldi, E. L.; Soler-Illia, G.; Grosso, D.; Cagnol, F.; Ribot, F.; Sanchez, C. *J. Am. Chem. Soc.* **2003**, *125*, 9770.

(7) Attard, G. S.; Bartlett, P. N.; Coleman, N. R. B.; Elliott, J. M.; Owen, J. R.; Wang, J. H. *Science* **1997**, *278*, 838.

(8) Ryoo, R.; Joo, S. H.; Kruk, M.; Jaroniec, M. *Adv. Mater.* **2001**, *13*, 677.

(9) Trikalitis, P. N.; Rangan, K. K.; Bakas, T.; Kanatzidis, M. G. *Nature (London)* **2001**, *410*, 671.

(10) Alberius, P. C. A.; Frindell, K. L.; Hayward, R. C.; Kramer, E. J.; Stucky, G. D.; Chmelka, B. F. *Chem. Mater.* **2002**, *14*, 3284.

(11) Grosso, D.; Soler-Illia, G.; Crepaldi, E. L.; Cagnol, F.; Sinturel, C.; Bourgeois, A.; Brunet-Bruneau, A.; Amenitsch, H.; Albouy, P. A.; Sanchez, C. *Chem. Mater.* **2003**, *15*, 4562.

(12) Severin, K. G.; Abdel-Fattah, T. M.; Pinnavaia, T. J. *Chem. Commun.* **1998**, 1471.

(13) Hyodo, T.; Abe, S.; Shimizu, Y.; Egashira, M. *Sens. Actuators, B* **2003**, *93*, 590.

(14) Yuliarto, B.; Zhou, H. S.; Yamada, T.; Honma, I.; Asai, K. *Chem. Lett.* **2003**, *32*, 510.

(15) Miyata, H.; Itoh, M.; Watanabe, M.; Noma, T. *Chem. Mater.* **2003**, *15*, 1334.

(16) Tate, M. P.; Hamilton, B. D.; Eggiman, B. W.; Wei, T. C.; Kowalski, J. D.; Hillhouse, H. W. Submitted for publication.

(17) Wanka, G.; Hoffmann, H.; Ulbricht, W. *Macromolecules* **1994**, *27*, 4145.

(18) Zhao, D. Y.; Huo, Q. S.; Feng, J. L.; Chmelka, B. F.; Stucky, G. D. *J. Am. Chem. Soc.* **1998**, *120*, 6024.

(19) Eggiman, B. W.; Tate, M. P.; Hillhouse, H. W. Submitted for publication.

(20) Falcaro, P.; Grosso, D.; Amenitsch, H.; Innocenzi, P. *J. Phys. Chem. B* **2004**, *108*, 10942.

(21) Brinker, C. J.; Lu, Y. F.; Sellinger, A.; Fan, H. Y. *Adv. Mater.* **1999**, *11*, 579.